

## CHAPTER 6

### Pre-Stack Simultaneous Inversion

The 3D seismic pre-stack simultaneous inversion applied for this project was a constrained sparse spike inversion (CSSI), and was applied using the RockTrace module in the Jason software. The workflow requires careful QC and appropriate parameter testing to optimize the final inversion results.

The objective of inversion parameter testing was to set the parameters and apply proper constraints to optimize the match between the resulting inverted elastic parameters and corresponding well logs as well as seismic and synthetic data. The QC panels in the RockTrace software consisted of several plotted graphs, showing the following information:

- Signal to noise ratio (dB) for all stacks: the curves represent the inverted signal to noise ratio, derived from the synthetic data and residual data for each stack separately.
- Well log correlation: curves represent the correlation between high-cut filtering well log and inverted trace for each of elastic parameters (acoustic impedance, shear impedance and density).
- Normalized inverted parameter cross-correlation: the three curves represent the cross-correlation between pairs of inverted elastic parameters minus the cross-correlation of the same parameters in the well log. A value close to 0 means that the elastic parameters show the same level of dependency as predicted by the well data.
- Well log normalized standard deviation: the three curves represent the standard deviation of the inverted trace normalized to the well log for the three elastic

parameters. This represents the dynamic of the inverted parameter compared to the well log data (optimal value should be close to 1).

- Sparseness: the three curves represent the contrast sparseness of the three elastic parameters.
- Combined misfit: a weighted combination of the 5 above.

The main parameters tests included; seismic misfit signal to noise ratio of near, mid and far angle stacks, contrast misfit acoustic impedance, shear impedance and density uncertainty and merge cut-off frequency (see CHAPTER 5). However, other parameters were set using default values (e.g. Gardner slope, mudrock slope, contrast misfit power, seismic misfit power, etc.).

Seismic misfit signal to noise ratio of all stacks were selected based on signal to noise ratio and a combined misfit in the QC panel. The minimum combined misfit with compromising high signal to noise ratio in dB were selected for near, mid and far angle stacks, respectively (Figures 6-1, 6-2 and 6-3).

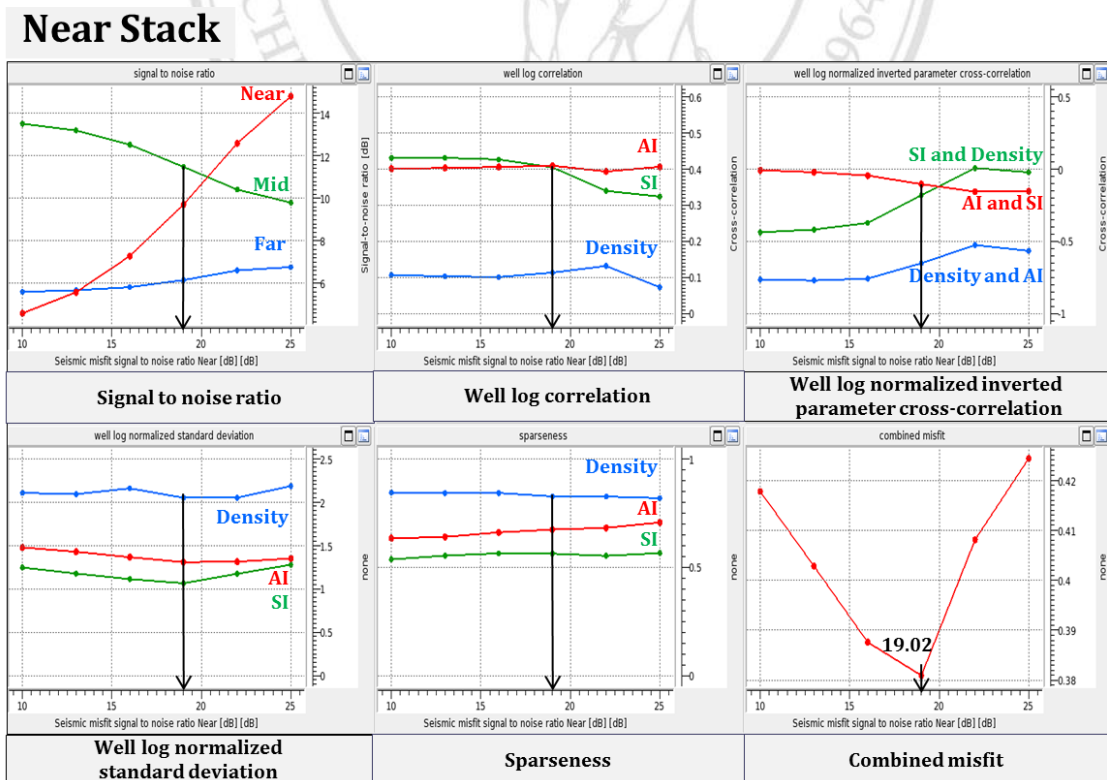


Figure 6-1 Seismic misfit signal to noise ratio of near angle stacks.

## Mid Stack

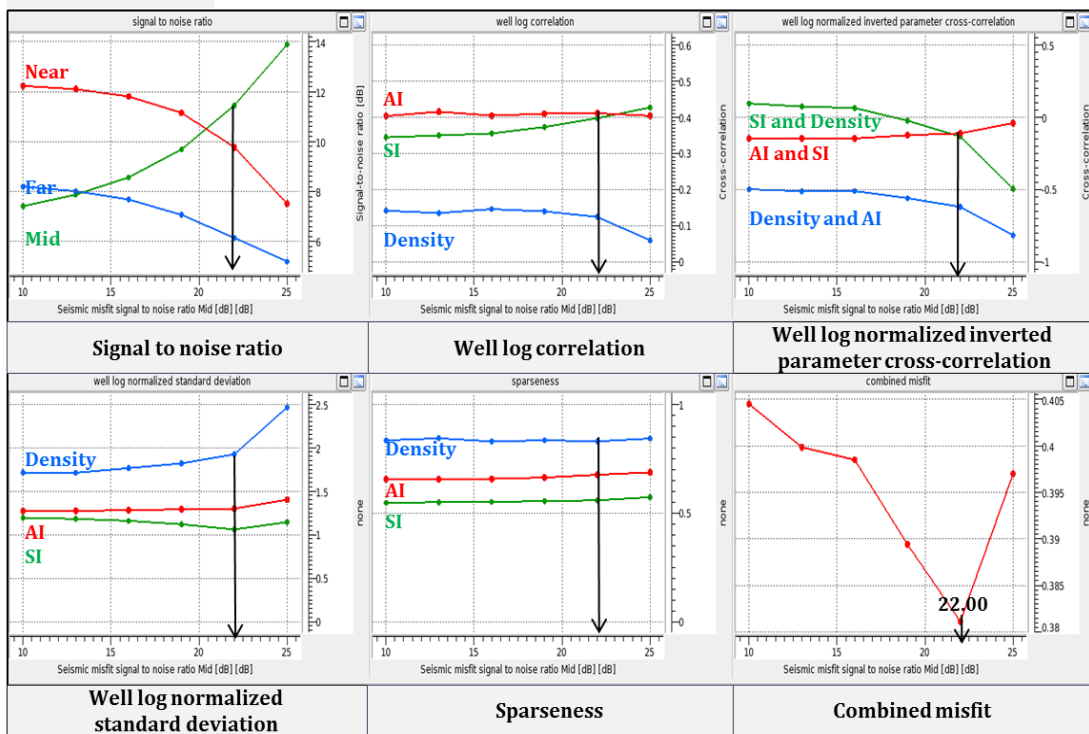


Figure 6-2 Seismic misfit signal to noise ratio of mid angle stacks.

## Far Stack

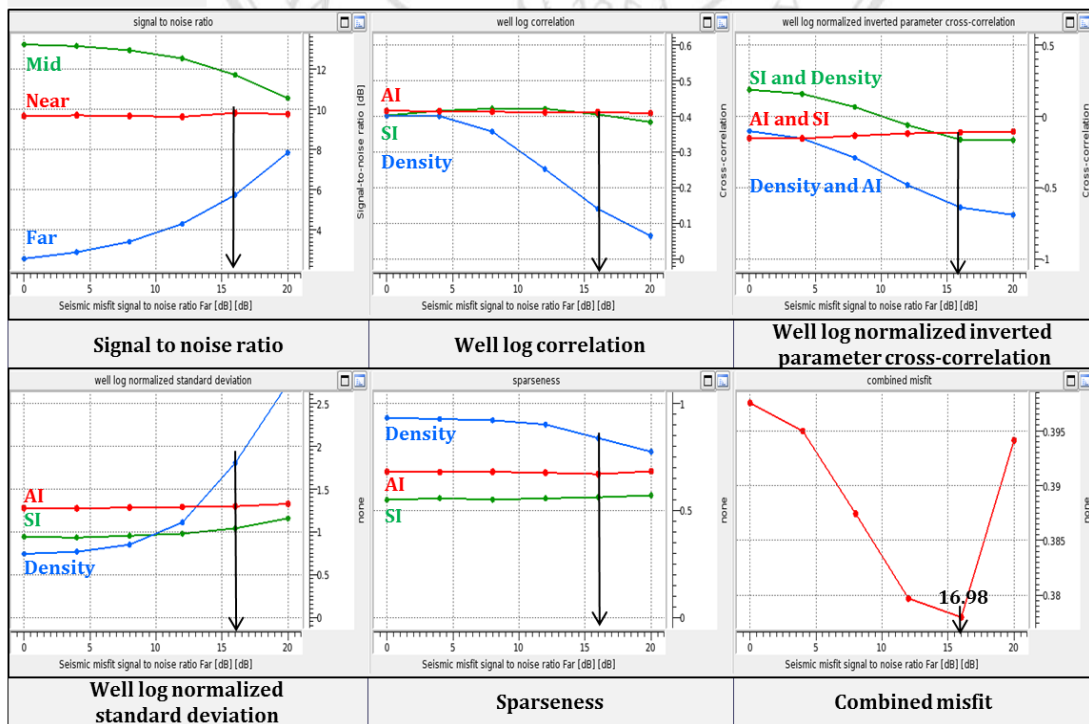


Figure 6-3 Seismic misfit signal to noise ratio of far angle stacks.

The graphs of well log correlation, well log normalized standard deviation and sparseness were integrated to achieve the contrast misfit acoustic impedance, shear impedance and density uncertainty. As comparing Figures 6-4 and 6-5, all graphs of contrast misfit acoustic impedance uncertainty were corresponded with contrast misfit shear impedance uncertainty. The contrast misfits were selected when well log correlation and well log normalized standard deviation graph were high (perfect = 1) and sparseness graph was optimum. However, QC panels of contrast misfit uncertainty for density were different from the ones for acoustic and shear impedances. It was difficult to reach a minimum on the combined misfit that benefited the parameters for density as the graphs relating to acoustic and shear impedances showed little of changing the contrast misfits (Figure 6-6). Based on the results of the QC panel analysis for each parameters, a final set of inversion parameters to be used in the study were summarized (Table 6-1).

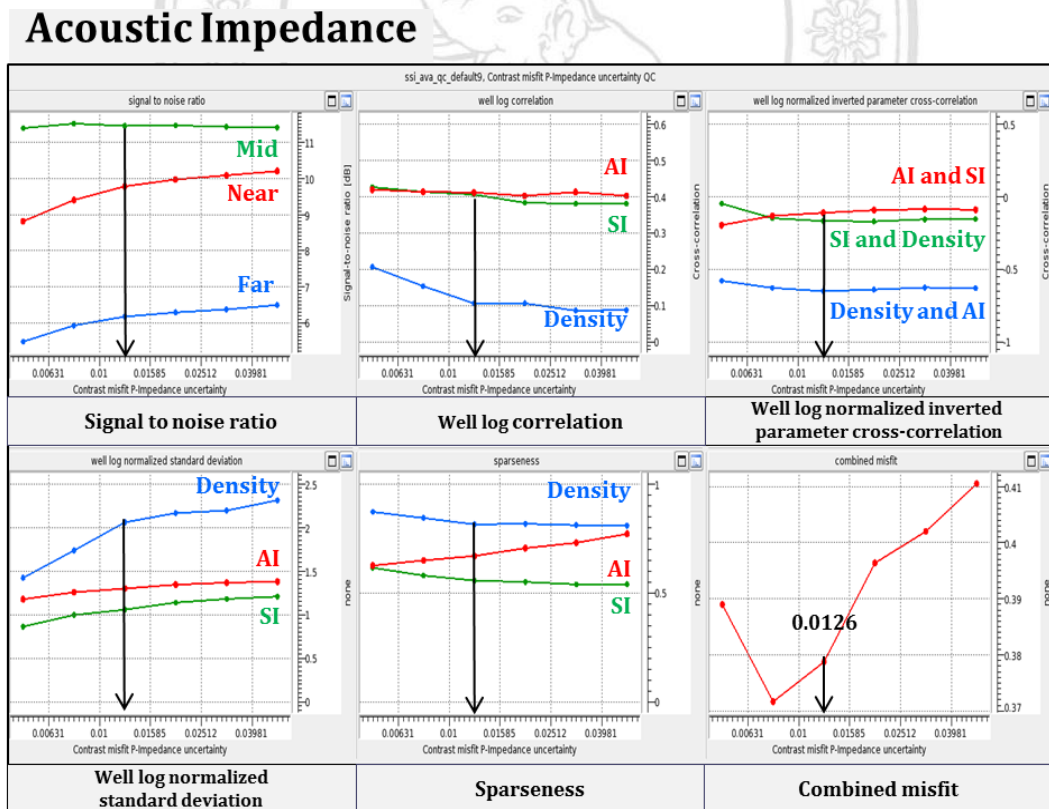


Figure 6-4 QC panel of contrast misfit acoustic impedance uncertainty.

# Shear Impedance

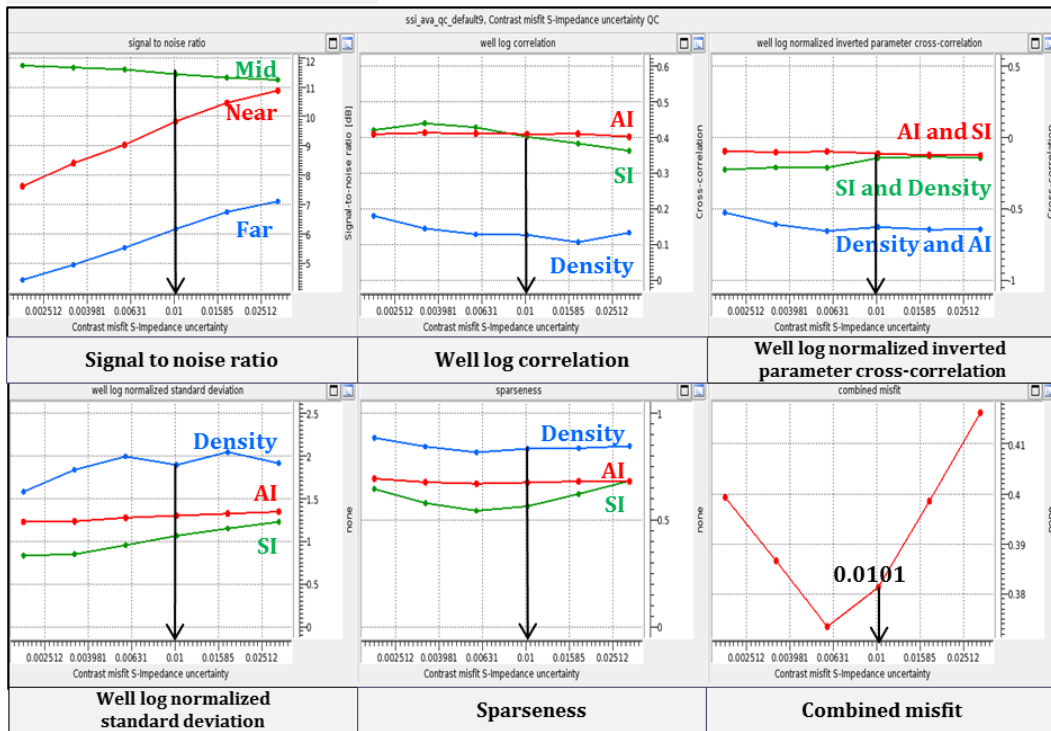


Figure 6-5 QC panel of contrast misfit shear impedance uncertainty.

# Density

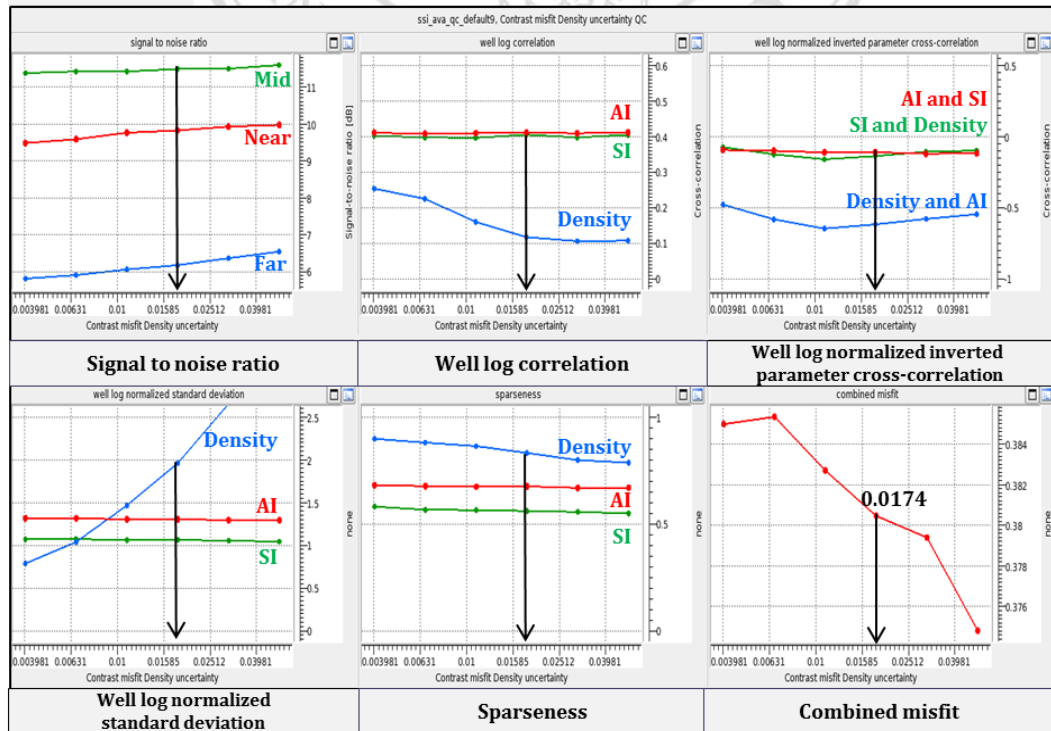


Figure 6-6 QC panel of contrast misfit density uncertainty.

Table 6-1 The final inversion parameters were used in the study.

<b>Seismic Inversion QC Parameters</b>	
Seismic misfit signal to noise ratio Near (dB)	19.02
Seismic misfit signal to noise ratio Mid (dB)	22
Seismic misfit signal to noise ratio Far (dB)	16.98
Contrast misfit P-impedance uncertainty	0.0126
Contrast misfit S-impedance uncertainty	0.0101
Contrast misfit density uncertainty	0.0174
Gardner slope	0.25
Mudrock slope	0.8620
Contrast misfit power	0.9
Seismic misfit power	2
Wavelet scale factor: Near	1
Wavelet scale factor: Mid	1
Wavelet scale factor: Far	1
Merge cutoff frequency	10
Rock physics equations cutoff frequency	6
Soft trend misfit multiplier	1

An arbitrary seismic line passing through all the input well locations was selected to be used for QC purposes (Figure 6-7). Seismic inversion products such as acoustic impedance, shear impedance,  $V_p/V_s$  and density were extracted along the random line. The results illustrate the variations in rock layer properties within the target interval from horizons H4 to H0. The frequency range included in the final absolute seismic inversion datasets was provided by the combined contribution of the low frequency model and the seismic frequency bandwidth. Bandpass filtering (10-11-55-60 Hz) was applied to the inverted elastic property data to remove the effect of the low frequency model, and produce relative elastic inversion datasets.

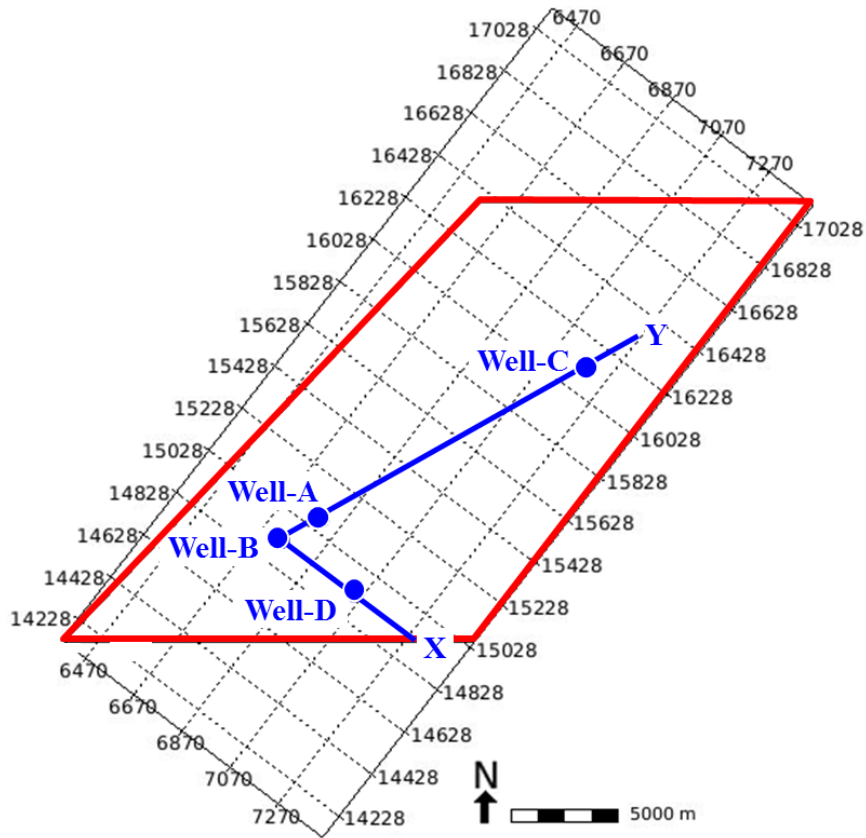


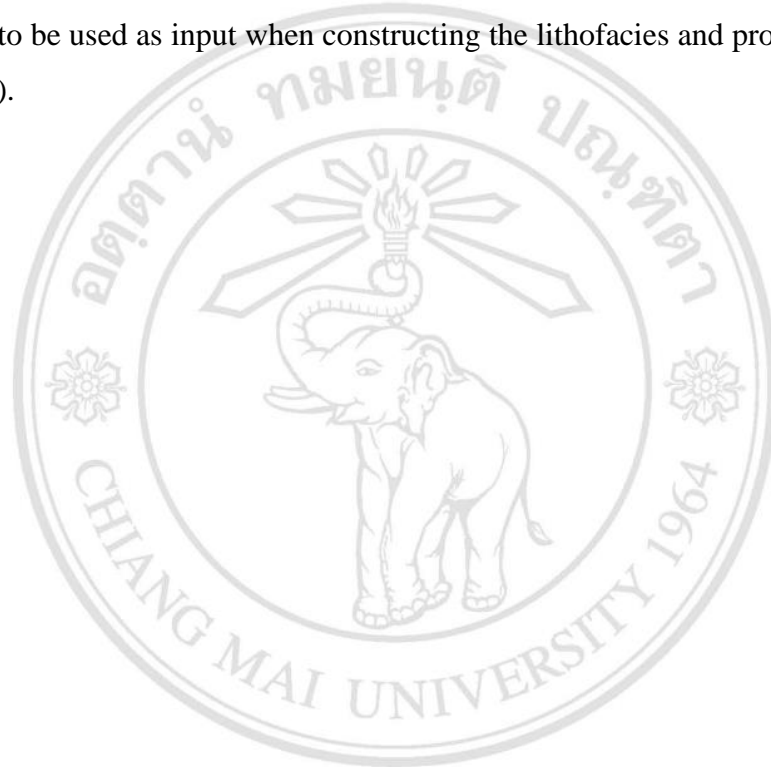
Figure 6-7 Index map showing arbitrary line.

The match between inverted elastic parameters for both absolute and relative seismic inversion cases were compared to the corresponding well log data, as shown in Figure 6-8 (acoustic impedance), Figure 6-9 (shear impedance), and Figure 6-10 ( $V_p/V_s$ ). As the relative inversion results were purely a product of the seismic input data, these were compared to bandpass-filtered logs. The QC showed that the acoustic impedance output was of good quality, and the shear impedance and  $V_p/V_s$  were of moderate to good quality. However, as ultra-far angle stack seismic data was not available, inverted density data was only considered to be of poor to moderate quality (Figure 6-11). (Additional results are available in APPENDIX C).

As part of the seismic inversion optimization, the final elastic parameter models should basically produce seismic data with noise-free when convolved with the seismic wavelets, also referred to as inverted synthetic data. As part of the QC of the seismic inversion results, residuals of each seismic partial stack (near, mid and far) were calculated by subtracting input seismic stacks from the inverted synthetic stacks.

Minimization of residuals was part of the seismic inversion criteria, and directly associated with the seismic signal to noise ratio. Results of derived residuals for near, mid and far angle stacks are shown in Figure 6-12.

Based on the result of the seismic simultaneous inversion testing, inverted acoustic impedance and  $V_p/V_s$  succeeded to optimize the match between the inverted elastic parameters and corresponding well logs, in addition to successfully minimizing the residuals. The final absolute acoustic impedance and absolute  $V_p/V_s$  3D volumes were decided to be used as input when constructing the lithofacies and probability cubes (see Chapter7).



ลิขสิทธิ์มหาวิทยาลัยเชียงใหม่  
Copyright© by Chiang Mai University  
All rights reserved



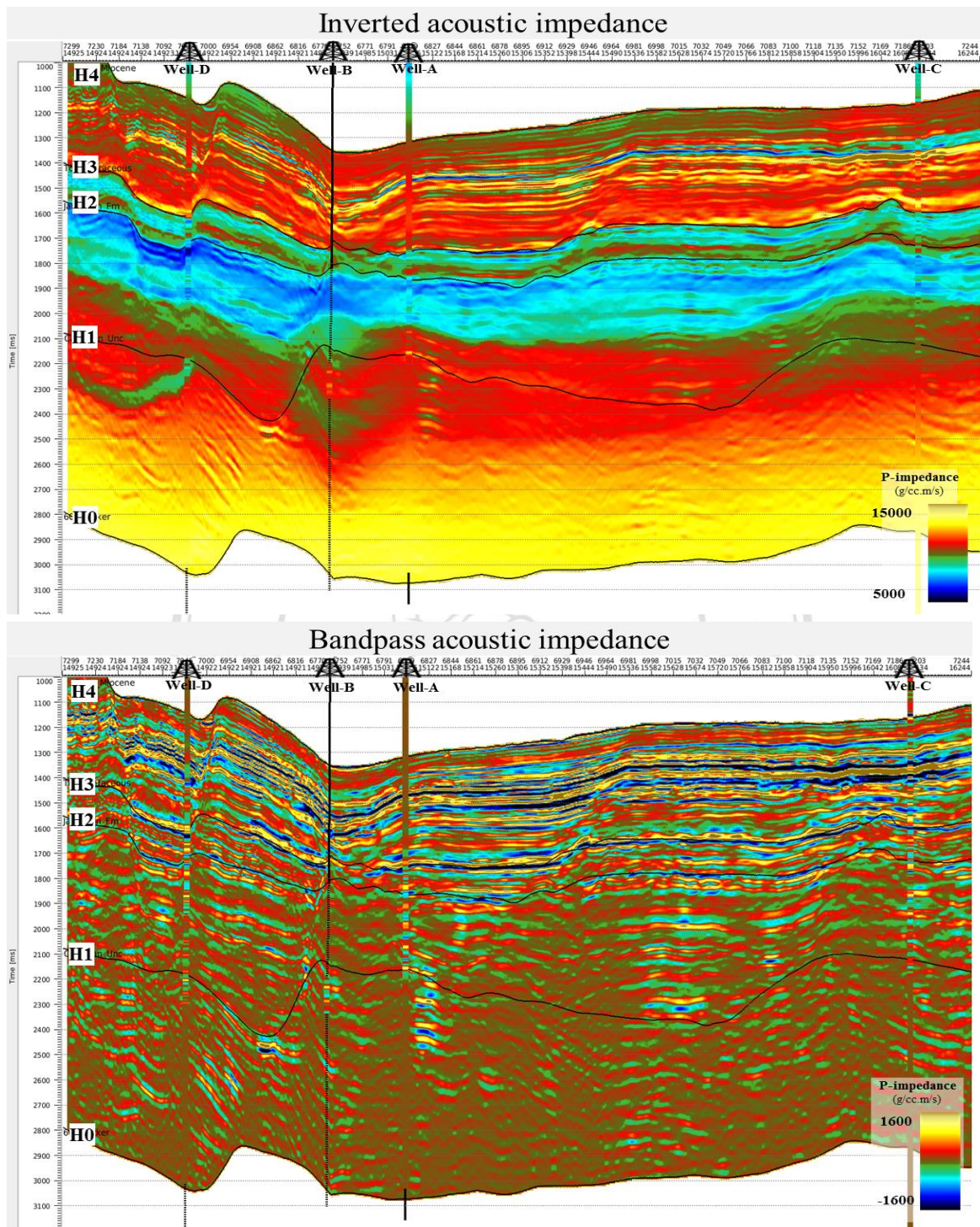


Figure 6-8 Final absolute acoustic impedance comparing with acoustic impedance logs at well location (top). Bandpass filtering were applied to both inverted acoustic impedance and well data to create comparable relative inversion results (bottom).

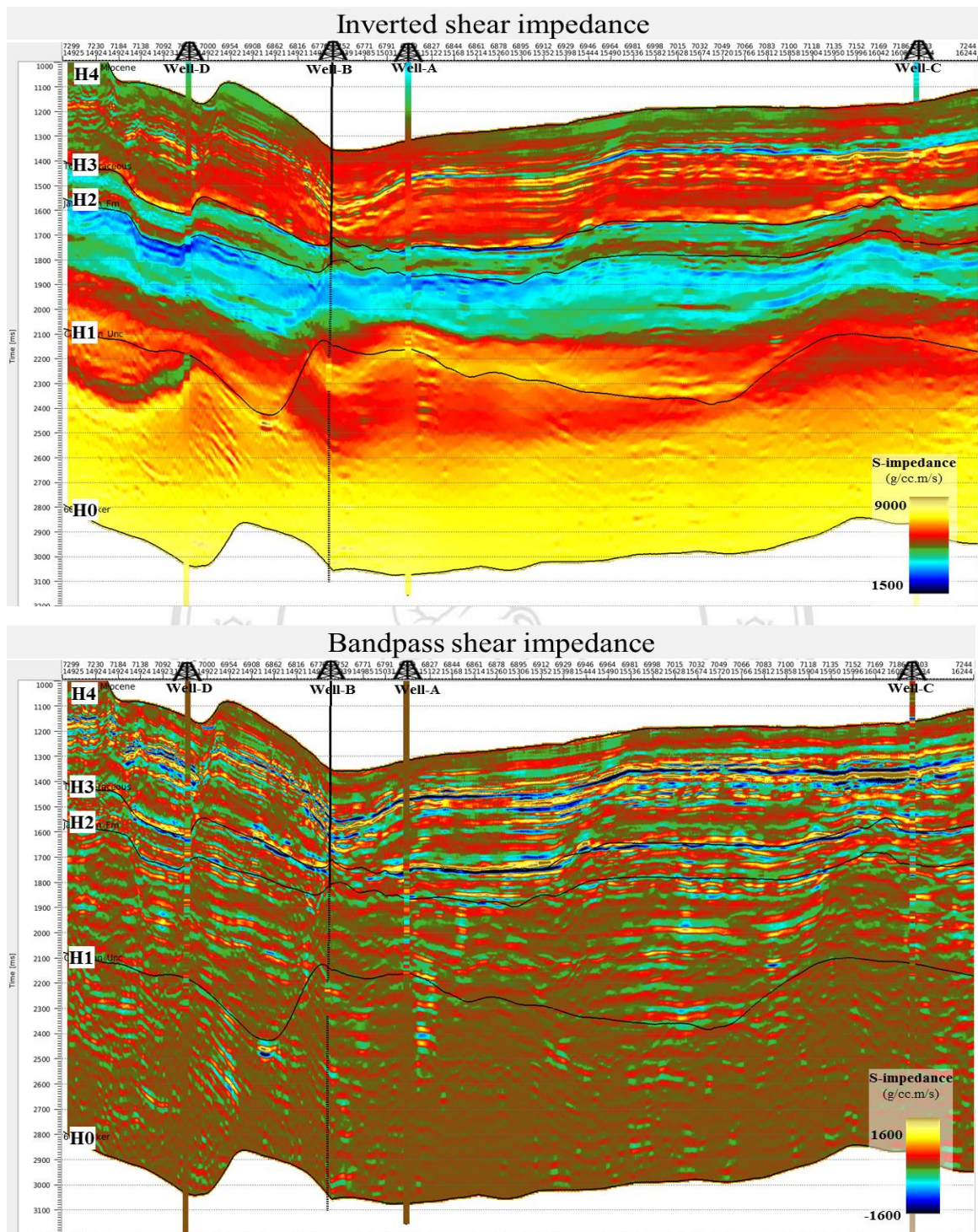


Figure 6-9 Final absolute shear impedance compared with shear impedance logs at well location (top). Bandpass filtering were applied to both inverted shear impedance and well log data to create comparable relative inversion results (bottom).

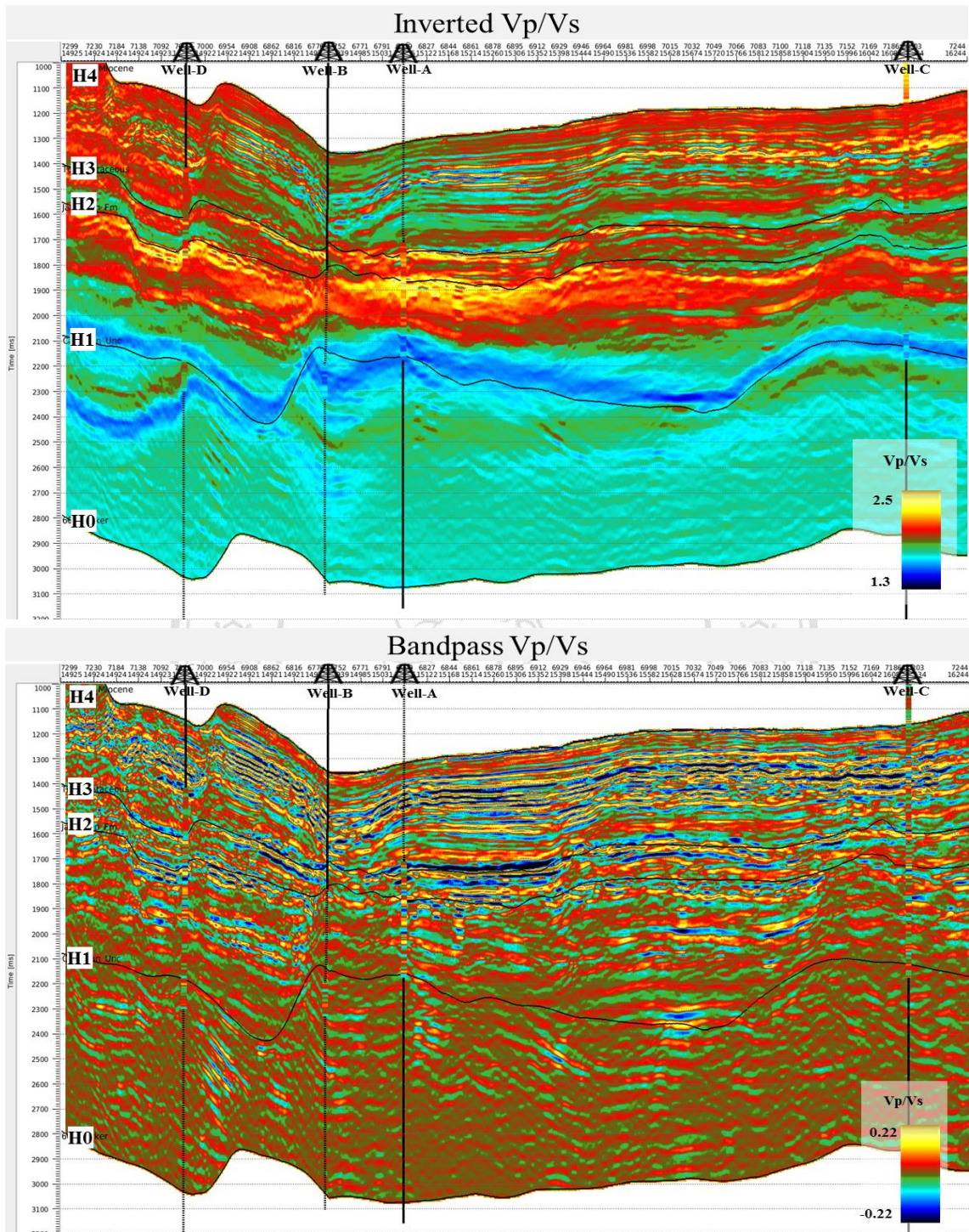


Figure 6-10 Final absolute Vp/Vs compared with Vp/Vs logs at well location (top). Bandpass filtering were applied to both inverted Vp/Vs and well log data to create comparable relative inversion results (bottom).

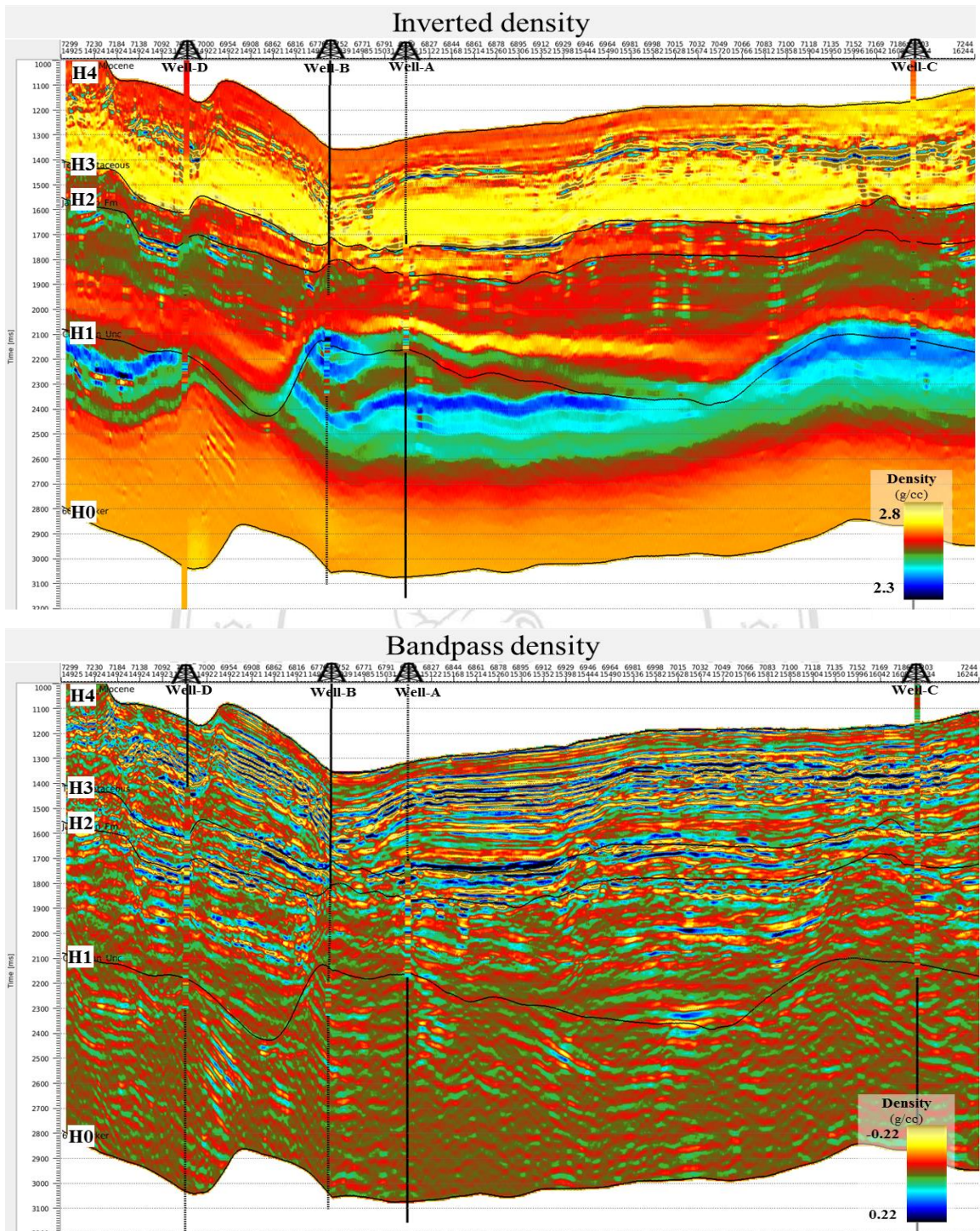


Figure 6-11 Final absolute density compared with density logs at well location (top). Bandpass filtering were applied to both inverted density and well log data to create comparable relative inversion results (bottom).

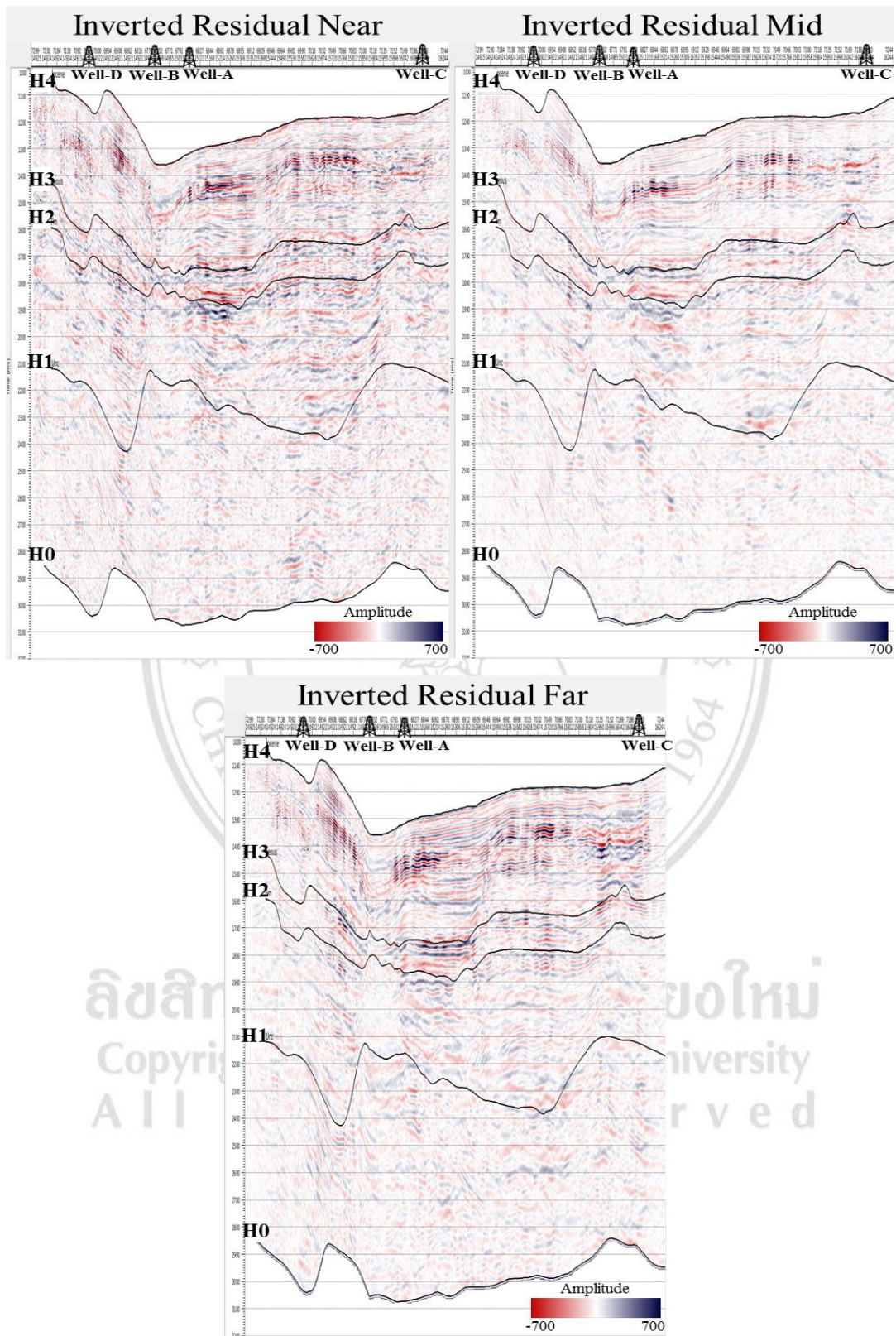


Figure 6-12 Derived residuals of near, mid and far angle stacks, achieved by subtracting input seismic data from inverted synthetic data.